J. Fluid Mech. (1984), *vol.* 142, *pp.* 39–55
Printed in Great Britain

Turbulence spectra from the viscous sublayer and buffer layer at the ocean floor

By T. M. CHRISS† AND D. R. CALDWELL
School of Oceanography, Oregon State University, Corvallis, Oregon 97331

(Received 19 April 1982 and in revised form 8 November 1983)

An experiment conducted on the Oregon continental shelf has provided measurements of velocity fluctuations in the viscous sublayer and buffer layer of the boundary-layer flow. Spectra from the viscous sublayer collapse considerably when scaled as suggested by Bakewell & Lumley (1967), and buffer-layer spectra collapse reasonably well with laboratory spectra when the scaling customarily used in the logarithmic layer is applied. However, in spite of the usefulness of the spectral scaling, the scaled sublayer and buffer-layer spectra from the ocean floor fall below the scaled laboratory spectra in the energy-containing portion of the spectrum, perhaps because the sea floor is not perfectly planar.

1. Introduction

One assumption often made in the study of boundary-layer turbulence is that measurements of mean and fluctuating quantities can be reduced to 'universal forms' when non-dimensionalized by characteristic length and velocity scales (Monin & Yaglom 1971, chap. 3). In earlier studies (Caldwell & Chriss 1979; Chriss & Caldwell 1983) we examined the hypothesis that the mean flow near the viscous sublayer of the bottom boundary layer on the Oregon continental shelf can be described as a universally similar, neutrally buoyant boundary-layer flow on a smooth wall. We concluded that, although the thickness of the viscous sublayer scales with ν/u_* as required by the concept of universal similarity, the scaling was not exact and the flow very near the bed is not quite as simple as smooth-walled flows in the laboratory. (Here u_* is the friction velocity and ν is the kinematic viscosity.) Nevertheless, in view of the many possible differences in circumstances (such as upstream conditions, freestream conditions, surface roughness or undulations, and temporal variability), the degree of agreement with laboratory studies is rather remarkable.

In this paper, we examine velocity spectra from a similar experiment in order to evaluate the hypothesis that spectra from the viscous sublayer and buffer layer of smooth-walled laboratory and geophysical flows can be reduced to universal forms by suitable non-dimensionalization. In addition, we examine the hypothesis that the gradient of non-dimensional velocity fluctuations in the viscous sublayer at the ocean floor is the same as in the laboratory.

† Present address: Department of Oceanography, Dalhousie University, Halifax, Nova Scotia, Canada B3H 4J1.

2. The experiment

The experiment was carried out on 9–10 June 1979 in 185 m water depth at 45° 20′ N on the Oregon continental shelf. The surface sediment is a silty sand (Runge 1966). The data were obtained from profiling heated-thermistor velocity sensors mounted on a 2 m high tripod placed on the sea floor. A digital data-acquisition system on the tripod sampled each thermistor once every 2 s. Additional instrumentation on the platform included temperature sensors, a Savonius rotor and a time-lapse cine camera which monitored the condition of the sensors.

Current was supplied to each thermistor to heat it approximately 20 °C above the water temperature. The temperature of a heated-thermistor sensor depends on the power dissipated in it and on the heat transferred away from the probe by the surrounding fluid. Because the calibration is a function of the water temperature and the orientation of the flow with respect to the thermistor, each thermistor was post-calibrated at the temperatures and flow directions observed during the experiment, by towing it in a 1 m radius annular channel. The power dissipated in the thermistor per unit change in temperature was related to the flow velocity by

$$P/\Delta T = a + bU^N, \tag{1}$$

where P is the power dissipated in the thermistor, ΔT is its temperature rise, U is the flow velocity, and a, b and N are experimentally determined. Inversion of this relationship allows the determination of current speed from values of $P/\Delta T$ computed from the output of the circuit (Caldwell & Dillon 1981). With this procedure, current speed can be determined with better than 0.1 cm s^{-1} accuracy in the laboratory. The water temperature varied only a few millidegrees while the data for a spectrum were being taken, so temperature contamination was not significant. The frequency response of these thermistors as velocity sensors has not been determined, but the same thermistors (Thermometrics Inc. Series FP14) have a -3 db point of 7 Hz when used as temperature sensors (Dillon & Caldwell 1980). Thus the frequency response of the velocity sensors was at least 7 Hz, far higher than necessary to resolve the Nyquist frequency, 0.25 Hz. The heated thermistors were used to determine the current speed only. Current direction was indicated by a small stationary vane.

The heated thermistors were mounted on a profiling arm carried up and down by a crank-and-piston mechanism driven by an underwater motor. The profiler mechanism was mounted 0.5 m outside one of the tripod legs, assuring unobstructed flow through an arc of 300°. Only periods of unobstructed flow were chosen for analysis. The profiling period was 213 min. The total vertical travel of the sensors was 6 cm. To ensure that the thermistors penetrated the viscous sublayer (at most a few cm thick), we allowed the thermistors to penetrate the sediment at the bottom of each profile. Their vertical position was determined within 0.03 cm by a potentiometer connected to the profiler motor. The position of the sediment–water interface was taken to be the zero-velocity intercept of the (linear) velocity profile within the viscous sublayer.

Although temperature microstructure data was not obtained during this experiment, profiles from a freely falling microstructure profiler at other times during the same cruise (Newberger & Caldwell 1981) indicate that the bottom few metres were within a few millidegrees of isothermal. The salinity gradient was not measured, but Caldwell (1978) found that, when the bottom layer was nearly isothermal, salinity variations were less than 0.002 parts per thousand and thus below the resolutions of the best instrumentation.

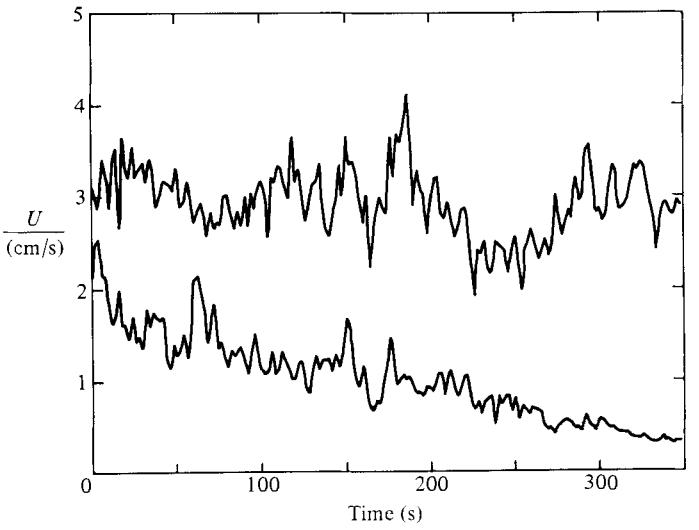

FIGURE 1. Typical time series from the viscous sublayer (lower series) and buffer layer (upper series). The series shown are not simultaneous. During the course of the sublayer series, the sensor moved from $y^+ = 6$ to $y^+ = 1$, accounting for the decrease in mean velocity. During the buffer layer series, the sensor moved from $y^+ = 22$ to $y^+ = 18$.

3. Data analysis

Two heated thermistors were separated horizontally by 11 cm and offset approximately 0.5 cm in the vertical. They penetrated the sediment by 4.5 and 5 cm, so we have current measurements from the lowest 1.5 cm of the water column. Based on the friction velocities $u_* = (\tau_0/\rho)^{\frac{1}{2}}$, which ranged from 0.15 to 0.36 cm s^{-1}, the sensor positions at the top of the profile corresponded to non-dimensional distances ($y^+ = yu_*/\nu$, where y is the height above the boundary) from $y^+ = 9$ to $y^+ = 29$. Each traverse from the top of the profile to the boundary took 2200 s. Because of the crank-and-piston mechanism, traverse speeds were slowest in the top millimetre of the profile (2.1×10^{-4} cm s^{-1}) and most rapid near the sediment (1.2×10^{-3} cm s^{-1}). At these speeds it required 400–700 s for the sensors to traverse from $y^+ = 0$ to $y^+ = 6$. Figure 1 shows typical time series in the viscous sublayer and in the buffer layer.

For each upward or downward traverse, a mean profile for the viscous sublayer was constructed by averaging the velocity measurements over 0.05 cm thick vertical intervals (figure 2). The shear in the sublayer was then used to compute the bed stress τ_0 by

$$\tau_0 = \rho\nu\frac{\partial\overline{U}}{\partial y}, \tag{2}$$

where ρ and ν are the density and kinematic viscosity of the fluid.

4. Spectra from the viscous sublayer

Given the magnitude of the mean flow and estimates of the typical magnitude of vertical and cross-stream velocity fluctuations in the viscous sublayer and buffer layer of laboratory flows (see e.g. Eckelmann 1974), it can be shown that, because of the nature of the vector addition process, the sensor responds almost exclusively to

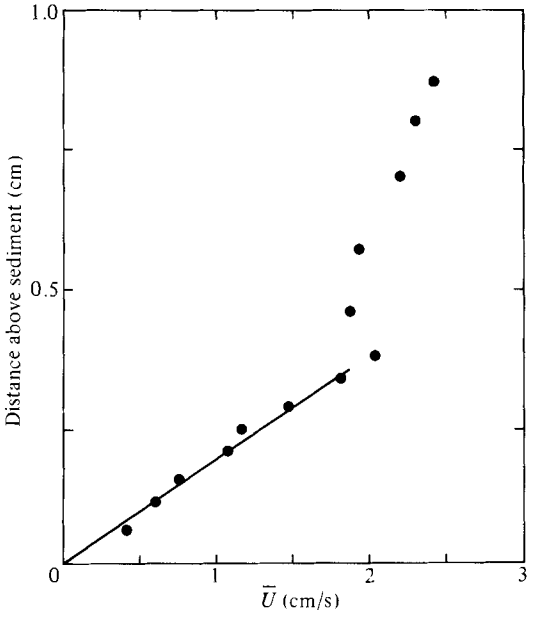

FIGURE 2. Typical mean-velocity profile. The straight line represents a linear fit to the data in the viscous sublayer.

streamwise fluctuations. At most a few percent of the energy is due to cross-stream contributions.

Ideally, spectra for the viscous sublayer would be computed over long periods with y^+ fixed. But, because of the self-contained nature of the instrumentation, the sensor positions could not be adjusted after the tripod left the deck of the ship. Because of this inability to set the position of the sensors precisely with respect to the boundary (owing to tripod settling, etc.) and because of the need to determine the shear in the sublayer (to obtain u_*) we allowed the sensors to move slowly through the sublayer hoping that this slow change of y^+ would not seriously influence the spectra. If the scaling suggested by Bakewell & Lumley (1967) is applicable then the shapes of the sublayer spectra (determined from the slowly moving sensor) should not differ from those from a fixed sensor.

Spectra were computed for seventeen 128-point series from the linear portion of the velocity profile. During the 256 s over which the spectra were computed, the sensor moved 0.2–0.3 cm, a y^+ change of 2–4. Prior to spectral analysis, the series were detrended to remove the effect of the velocity gradient. Power spectral densities SD (f) defined by

$$u'^2 = \int_0^\infty \mathrm{SD}\,(f)\,\mathrm{d}f \tag{3}$$

were computed using a fast-Fourier-transform algorithm. In (3), u' is the r.m.s. value of the streamwise velocity fluctuation. After computation, the raw estimates were band-averaged, with more estimates being included in the bands at higher frequencies.

Typical sublayer spectra are shown in figure 3. Bakewell & Lumley (1967) and Ueda & Hinze (1975) present spectra from the viscous sublayer of laboratory flows in which the fluids and the flow conditions were significantly different from those in the ocean.

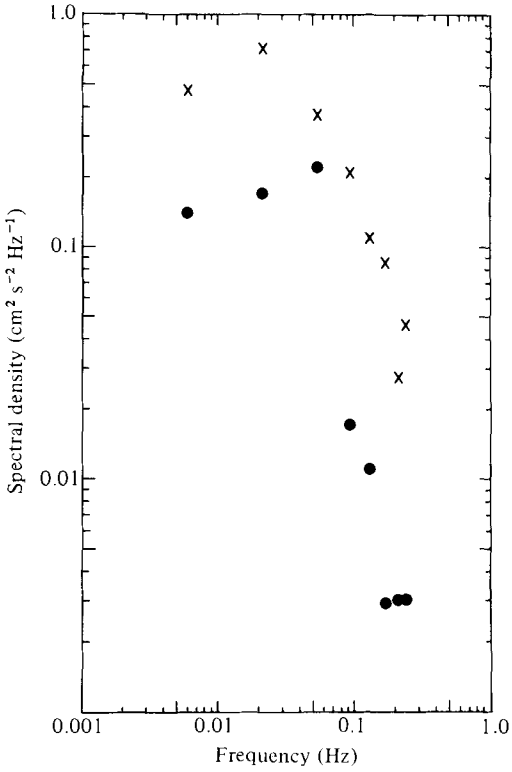

FIGURE 3. Typical spectra from the viscous sublayer: ×, $u_* = 0.28$ cm s^{-1}, $y^+ = 4.6$; ●, $u_* = 0.28$ cm s^{-1}, $y^+ = 3.6$. Confidence intervals are the same as those shown in figure 4.

Bakewell & Lumley's are from turublent pipe flow of glycerol ($\nu = 2.18$ cm^2 s^{-1}), whereas the Ueda & Hinze data come from a wind tunnel ($\nu = 0.151$ cm^2 s^{-1}). The friction velocities were 50 and 39.1 cm s^{-1} respectively. The unscaled spectra from these studies are quite different from ours (figure 4). (Computational errors apparently crept into the spectral plots presented in both laboratory studies. Bakewell & Lumley's spectra integrate to 2π times the variance determined from other figures in their paper, while those of Ueda & Hinze integrate to 76 times the variance. We have adjusted the spectral densities of the two laboratory studies by dividing by 2π and 76 respectively.)

Bakewell & Lumley propose that sublayer spectra can be reduced to a single curve if frequencies $\omega = 2\pi f$ are non-dimensionalized by ν/u_*^2 and spectral densities are non-dimensionalized by ωy^2. Their spectra for three different y^+ within the sublayer are collapsed by this scaling to a single curve. Because u_* and ν were not varied in Bakewell & Lumley's experiment, the collapse of their spectra to a single curve does not imply that the scaling of frequency is correct. A test of the frequency scaling requires data from flows in which ν/u_*^2 varies significantly. Based on the viscosity of seawater (0.015 cm^2 s^{-1}) and the range of u_* in our experiment, ν/u_*^2 is up to 470 times larger than in Bakewell & Lumley's experiment and up to 11 000 times larger than in the Ueda & Hinze experiment. The spectra from the three experiments thus furnish an excellent opportunity to test the scaling proposed by Bakewell & Lumley.

Before applying the proposed scaling, consider the effect of sensor motion on the

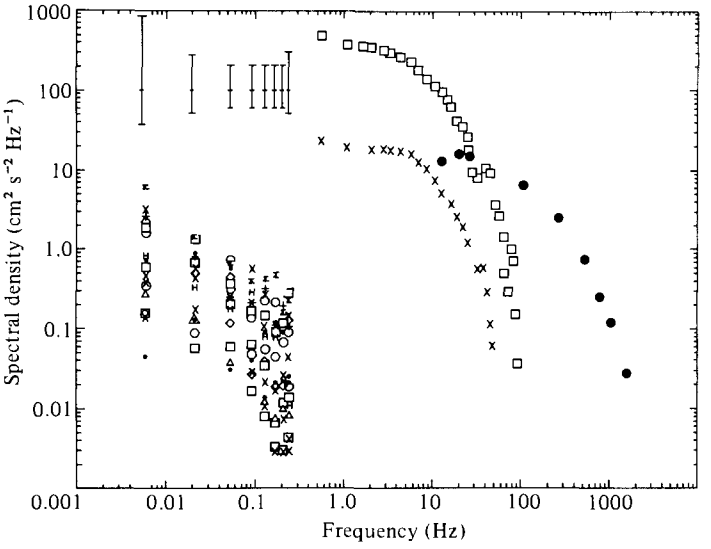

FIGURE 4. Sublayer spectra from our study (at left) plotted with sublayer spectra from the laboratory studies of Bakewell & Lumley (1967) and Ueda & Hinze (1975). The Bakewell & Lumley spectra are for $y^+ = 1.25$ (×) and $y^+ = 5$ (□). The Ueda & Hinze spectrum (●) is for $y^+ = 3$. Confidence limits shown for our spectra are 95% confidence limits assuming a chi-square distribution (Bath 1974). Symbols and flow conditions for our spectra are given in table 1. Where several symbols coincide, one or more have occasionally been deleted for clarity.

Symbol	Data interval	u_* (cm/s)	y^+
Σ	1	0.36	5.0
×	16	0.27	5.1
+	2	0.26	6.0
◇	4	0.29	5.5
□	17	0.24	5.7
○	6	0.26	6.6
H	8	0.19	4.8
●	15	0.30	6.0
□	12	0.15	5.6
×	3	0.28	4.6
×	10	0.17	5.3
○	7	0.26	2.7
△	13	0.17	3.7
□	11	0.15	3.3
◇	5	0.19	3.7
×	9	0.17	3.6
●	14	0.17	4.0

TABLE 1. Flow conditions for ocean floor spectra presented in figure 4. Note that the symbols are ordered vertically in the same sequence that they appear in the lowest frequency estimate of figure 4.

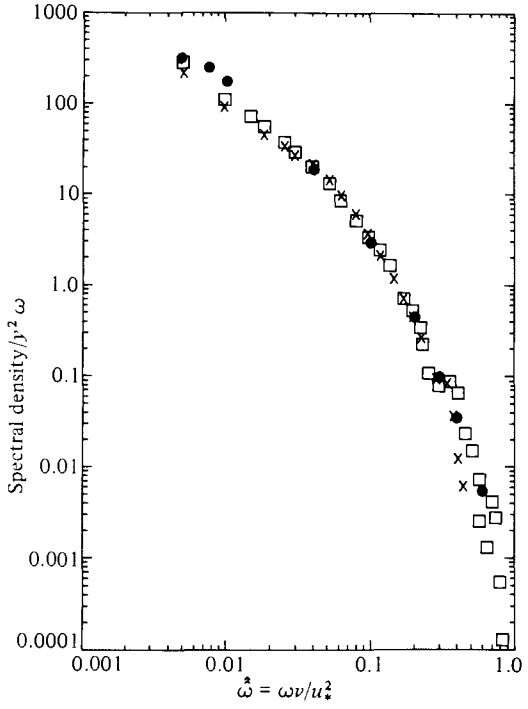

FIGURE 5. Scaled sublayer spectra from Bakewell & Lumley (1967) and Ueda & Hinze (1975). Symbols are the same as in figure 4.

computed spectrum. If u_* is constant and the scaling proposed by Bakewell & Lumley holds, then for fixed ν and u_* the non-dimensional spectral density $\widehat{\mathrm{SD}} = \mathrm{SD}\,(\omega)/y^2\omega$ depends only on the non-dimensional frequency $\hat{\omega} = \omega\nu/u_*^2$. Thus, with fixed ν and u_*, the dimensional spectral density $\mathrm{SD}\,(\omega)$ at dimensional frequency ω should equal $c(\omega)\,y^2$, where $c(\omega)$ is a proportionality constant depending only on ω. A sensor moving at a constant velocity from $y = y_1$ to $y = y_2$ observes a spectral density at frequency ω given by

$$\mathrm{SD}\,(\omega) = (y_2 - y_1)^{-1} \int_{y_1}^{y_2} c(\omega)\, y^2\, \mathrm{d}y, \tag{4}$$

which is equivalent to $c(\omega)\, y_3^2$, where y_3 is given by

$$y_3^2 = \frac{y_2^3 - y_1^3}{3(y_2 - y_1)}. \tag{5}$$

So, if the scaling proposed by Bakewell & Lumley is valid, the spectrum calculated from a time series obtained from a sensor that moves from y_1 to y_2 should be identical with the spectrum that would have been obtained from a fixed sensor at y_3 (providing that the time series had first been detrended to remove the variance resulting from moving through a mean velocity gradient). We have used the lowest and highest positions of the thermistor during the series to calculate y_3 for non-dimensionalizing our spectra.

In figures 5 and 6 we present scaled versions of the spectra of figure 4. Although the result is not perfect, the scaling does collapse the spectra considerably. Much of the scatter at the low-frequency end of our data may reflect the fact that each point

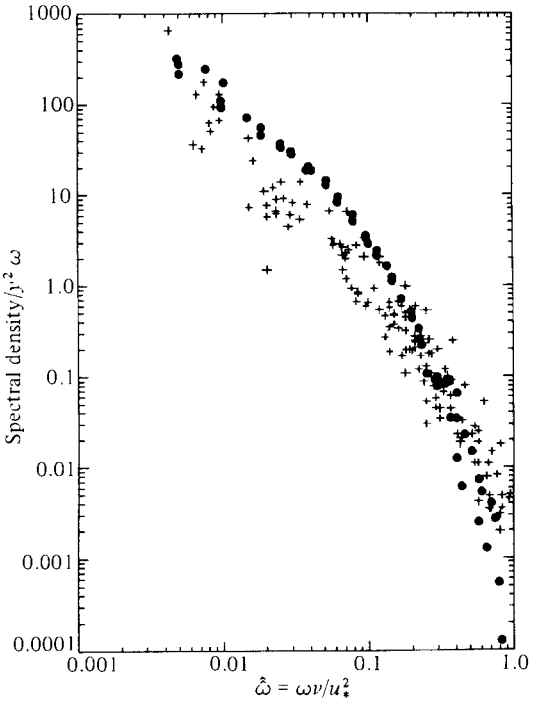

FIGURE 6. Scaled spectra from our study together with those of the two laboratory studies. In this figure all laboratory points are shown by solid circles.

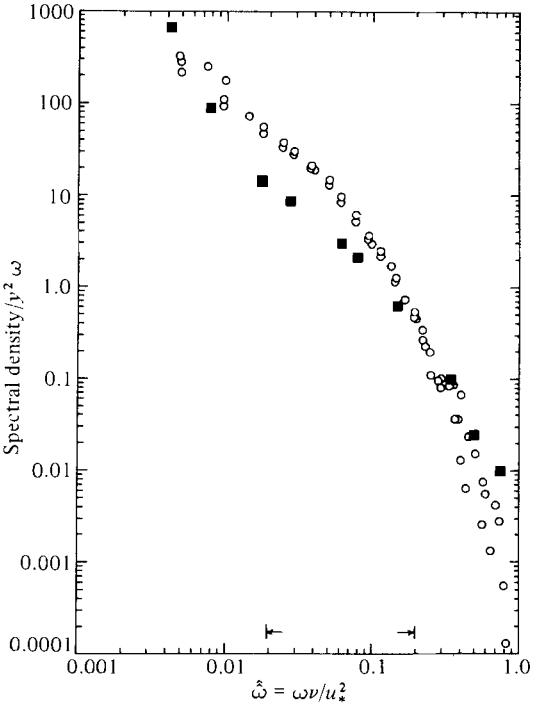

FIGURE 7. Ensemble-averaged spectrum from our study (■) plotted with the laboratory spectra (○). The spectral estimate for the lowest frequency is based on only one data point in the averaging band and therefore is not as well determined as the other estimates. The horizontal arrows delimit the energy-containing range of the laboratory spectra.

represents only a single spectral estimate. Ensemble-averaged spectra (figure 7) compare very well with the laboratory spectra except within the non-dimensional frequency range 0.01–0.08 where our spectra show slightly less energy.

We tried a Kolmogoroff scaling in which the timescale is ν/u_*^2 and the lengthscale is ν/u_*. Under this scaling the dimensionless frequency is $\omega\nu/u_*^2$, as in the Bakewell–Lumley scaling, but the dimensionless spectral density is SD/ν. The points from the various studies collapsed pretty well in frequency, of course, but not nearly as well in the SD-axis. Therefore y appears to be the significant lengthscale for $y^+ \leqslant 7$.

The agreement of the non-dimensional spectra from the three experiments (figure 7) is strong support for the validity of the scaling proposed by Bakewell & Lumley. Despite the potentially greater complexity of the geophysical boundary-layer flow, the viscous sublayer at the ocean floor behaves substantially like its laboratory counterpart in this respect.

5. The vertical structure of the streamwise velocity fluctuations in the viscous sublayer

A number of laboratory studies have examined the dependence of the r.m.s. streamwise velocity fluctuation u' on y^+ (Eckelmann 1974; Mitchell & Hanratty 1966; Hanratty 1967; Ueda & Hinze 1975; Kreplin & Eckelmann 1979). The laboratory data suggest that u'/u_* is roughly proportional to y^+ between $y^+ = 1$ and $y^+ = 5$, but the value of the proportionality constant varies from study to study. Mitchell & Hanratty (1966) summarize early determinations (Laufer 1951, 1954; Klebanoff 1954), which show a large variability (from 0.21 to 0.44), but more recent determinations (Comte-Bellot 1965; Mitchell & Hanratty 1966; Bakewell & Lumley 1967; Hanratty, Chorn & Hatziarramidis 1977; Ueda & Hinze 1975; Eckelmann 1974; Kreplin & Eckelmann 1979) typically yield values between 0.30 and 0.38. Kreplin & Eckelmann suggest that the value of the 'constant' varies with y^+ and decreases from 0.38 at $y^+ = 4.5$ to 0.32 at $y^+ = 1.5$. In contrast with the above results, which suggest no obvious influence of Reynolds number, Coantic (1967) indicates that $u'/u_* y^+$ decreased from 0.31 to 0.21 as the Reynolds number in his experiments was increased from 50000 to 450000. Using flush-mounted hot-film wall sensors, Eckelmann (1974), Kreplin & Eckelmann (1979), and Sreenivasan & Antonia (1977) obtained estimates of 0.24–0.25 for the limiting value of the constant at the wall, although Py (1973) and Fortuna & Hanratty (1971), using electrochemical wall-stress sensors, obtained 0.3 at the wall. Because the limiting value of the constant is approximately equal to the ratio of the r.m.s. fluctuating wall stress to the mean wall stress (Eckelmann 1974), its value may be relevant to sediment-transport studies.

We have determined u' for each of the 128-point sublayer time series. For the 17 series $u'/u_* y^+$ is 0.20 ± 0.03 (standard deviation). To resolve 99 % of the variance in Bakewell & Lumley's sublayer spectrum, the spectra must include the non-dimensional frequency band from 4.6×10^{-3} to 4.2×10^{-1}. Although our ensemble average spans this energy-containing band (figure 7), each individual 128-point spectrum does not. Depending on the value of u_*, each 128-point spectrum missed predominantly either the high-frequency or the low-frequency end of the energy-containing range. Given the largest and smallest non-dimensional frequencies resolved in each spectrum, we find that the individual spectra would have resolved from 76 % to 90 % of the energy in the Bakewell & Lumley spectrum. Thus the ratio $u'/u_* y^+$ calculated from our data is likely to be too low. After using the Bakewell & Lumley spectrum to correct for these effects, $u'/u_* y^+$ becomes 0.21 ± 0.03. Even after correction, our sublayer spectra contain less energy than expected from laboratory results.

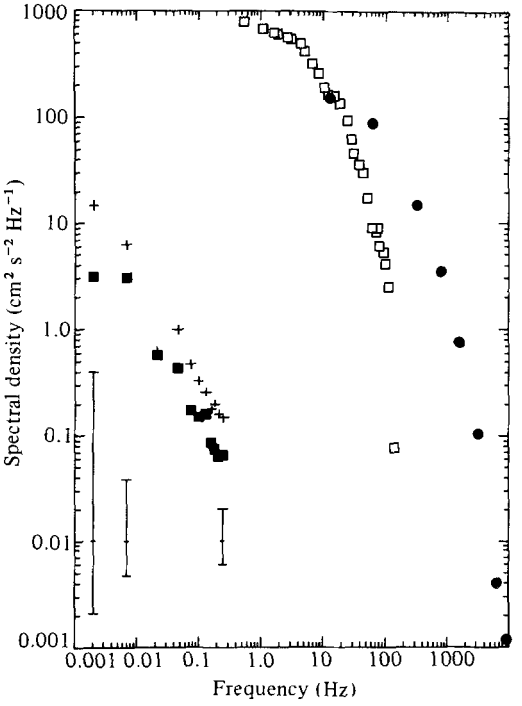

FIGURE 8. Typical buffer-layer spectra from our study (■, $u_* = 0.19$ cm s^{-1}, $y^+ = 19$; +, $u_* = 0.26$ cm s^{-1}, $y^+ = 29$) plotted with laboratory buffer-layer spectra of Bakewell & Lumley ($y^+ = 20$, □) and Ueda & Hinze ($y^+ = 21$, ●). Confidence limits not shown are the same as for the highest frequency estimate of our study.

6. Spectra from the buffer layer

The buffer-layer spectra were computed for five 256-point series, selected so that the sensor was within the top millimetre of the traverse and y^+ was greater than 18. For these intervals y^+ varied from 18 to 29, depending on u_*. With the very slow traverse speeds at the top of the profile, the sensors moved only 1–1.2 non-dimensional units during the 512 s over which a spectrum was computed. Laboratory data suggest little change in the turbulence structure over this distance, so the profiler motion should not influence the buffer-layer spectra. To remove the effect of any trend in mean velocity, the series were detrended before analysis.

Figure 8 shows two representative buffer-layer spectra ($y^+ = 19$ and $y^+ = 29$) from our study, along with buffer-layer spectra ($y^+ = 20$ and $y^+ = 21$) from Bakewell & Lumley (1967) and Ueda & Hinze (1975). To our knowledge no spectral scaling has been proposed for buffer-layer velocity spectra. Because u'/u_* varies by no more than 30 % between $y^+ = 18$ and $y^+ = 30$ (Bakewell & Lumley 1967; Kreplin & Eckelmann 1979; Ueda & Hinze 1975), Bakewell & Lumley's spectral scaling for the viscous sublayer (which depends strongly on y^2) cannot work for buffer layer spectra, so we sought another scaling. In the logarithmic layer of atmospheric and laboratory flows, it is common to non-dimensionalize the frequency axis by $y/\bar{U}(y)$ (where $\bar{U}(y)$ is the mean velocity) and to non-dimensionalize the spectral densities by u_*^2/ω. We have applied this scaling to the two sets of laboratory data (figure 9). Rather than dividing the spectral density by u_*^2/ω as is commonly done, we have divided by $u_*^2\,\hat{\omega}/\omega$, where $\hat{\omega}$ is the non-dimensional frequency. This non-dimensionalization is not fundamentally

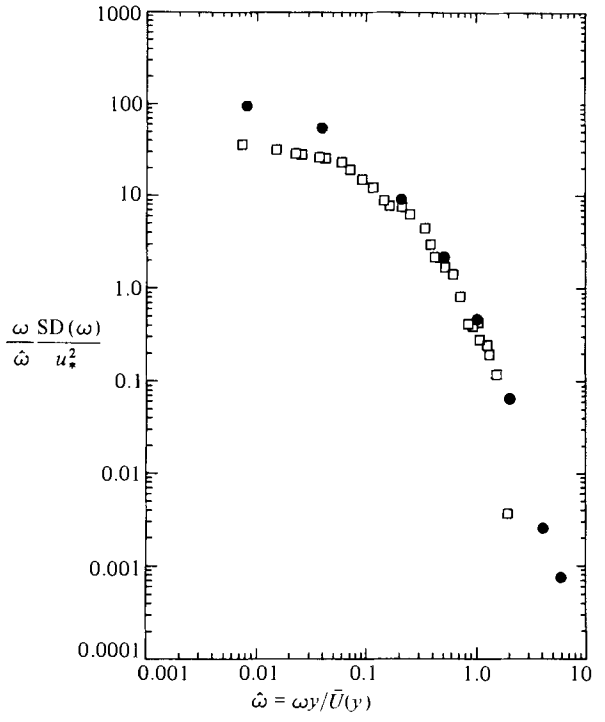

FIGURE 9. Scaled versions of the laboratory buffer-layer spectra shown in figure 8. Symbols are the same as in figure 8.

different, but has the advantage that the shape of the scaled and unscaled spectra remain the same. Except for the lowest frequencies, the proposed scaling does collapse the laboratory data to a single curve. It should be noted that, because the two sets of laboratory data have substantially the same y^+, we cannot argue that the proposed scaling is independent of y^+. Since the Reynolds numbers of the two laboratory experiments differed by an order of magnitude, it appears that the scaling does not depend strongly on Reynolds number in this range.

One difficulty in applying the proposed scaling to our spectra is that, because we cannot measure the shear in the sublayer when the sensors are in the buffer layer, we lack u_* measurements simultaneous with the buffer-layer spectra. A stationary Savonius rotor on the platform indicates that the 'mean' flow was not always constant between the time the sensors were in the sublayer and the time they were at the top of the profile. We have therefore estimated u_* from the current speeds determined by the rotor in the logarithmic layer. In doing so, we have assumed the commonly accepted value of 11.6 for the non-dimensional sublayer thickness δ^+ even though an earlier study (Chriss & Caldwell 1983) indicates that δ^+ may vary from this value in the marine environment. (Because of the profiling scheme, determinations of δ^+ were not possible in the present study.) Chriss & Caldwell (1983) show that u_* determinations based on log layer velocities and the assumption that $\delta^+ = 11.6$ may differ by as much as 30 % from u_* values determined from sublayer data. Thus using the rotor to estimate u_* may introduce some error into the non-dimensional spectra.

In figure 10 we present scaled versions of our buffer-layer spectra ($18 < y^+ < 29$) along with those from the two laboratory studies. Comparing with figure 8, one can

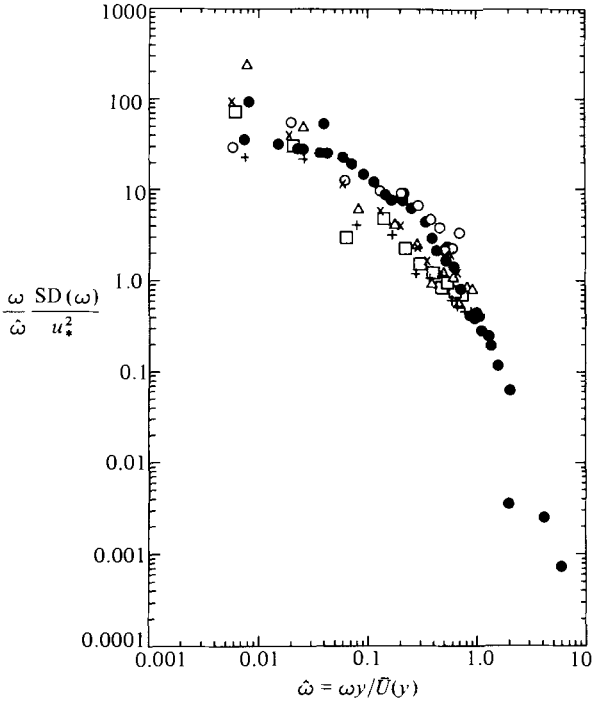

FIGURE 10. Scaled buffer-layer spectra from our study plotted with those of the two laboratory studies. The laboratory spectra are shown with solid circles. △, $u_* = 0.19$ cm s^{-1}, $y^+ = 19$; ×, $u_* = 0.26$ cm s^{-1}, $y^+ = 29$; □, $u_* = 0.26$ cm s^{-1}, $y^+ = 29$; ○, $u_* = 0.18$ cm s^{-1}, $y^+ = 18$; +, $u_* = 0.19$ cm s^{-1}, $y^+ = 19$.

see that the scaling is relatively successful, particularly considering the uncertainties in the u_* estimates for our spectra. The shape of our ensemble-averaged spectrum (figure 11) is similar to those from the laboratory except that both ours and that of Ueda & Hinze (1975) show a slightly more extensive -1 power-law range than does the spectrum of Bakewell & Lumley (1967).

7. Discussion

Although the proposed spectral scaling works reasonably well in both the viscous sublayer and the buffer layer, the spectra from the ocean floor fall below the laboratory spectra in the energy-containing portion of the non-dimensional frequency band (figures 7 and 11). (The horizontal arrows in these figures delimit the frequency band that contains 80% of the variance of the streamwise velocity fluctuations in the laboratory data.) Although the fact that our non-dimensional buffer-layer spectra fall below the laboratory spectra may be caused by errors in estimating u_*, it is also possible that the deviations from the laboratory spectra may reflect real differences in the flows.

One possible explanation is that the laboratory spectra may be Reynolds-number dependent, as suggested by Coantic (1967). It is difficult to compute a Reynolds number for our experiment because our highest measurements were in the logarithmic layer (within a metre of the seabed) and thus we have no measurement of the boundary-layer thickness or the freestream velocity. However, if we use the thickness

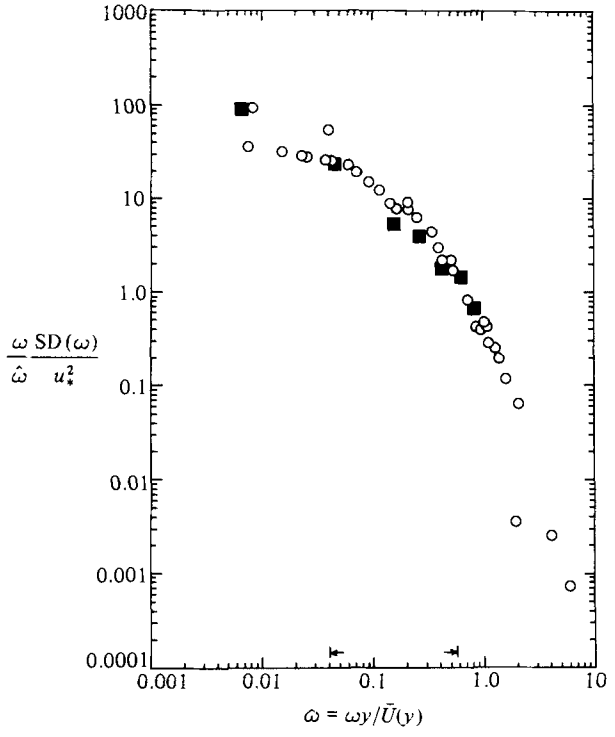

FIGURE 11. Ensemble-averaged buffer-layer spectrum from our study (■) plotted with laboratory buffer-layer spectra (○). The horizontal arrows delimit the energy-containing range of the laboratory spectra.

(5–10 m) of the bottom mixed layer (Newberger & Caldwell 1981; Caldwell 1978) to estimate the boundary-layer thickness, and take the freestream velocity to be approximately $30u_*$, the Reynolds number would be approximately 250000–500000 for typical u_* values (0.25 cm/s) in our experiment. Thus, if we accept Coantic's finding that u'/u_*y^+ is Reynolds-number dependent, our finding of $u'/u_*y^+ = 0.21$ is not unreasonable.

One difficulty with this explanation is that we are aware of only three investigations in which u'/u_*y^+ has been measured at very high Reynolds number, and these studies do not agree about the Reynolds-number dependence. Laufer (1954) conducted turbulent-pipe-flow experiments at $Re = 50000$ and 500000 and found no Reynolds-number dependence. Comte-Bellot (1965) measured u'/u_*y^+ in a turbulent channel flow at three Reynolds numbers from 57000 to 230000 and also found no Reynolds-number dependence. Thus the systematic decrease from 0.31 to 0.21 found by Coantic (1967) as the Reynolds number was increased from 50000 to 450000 is somewhat puzzling. The Reynolds-number dependence found by Coantic may be related to spatial averaging by his hot-wire anemometers. In a recent study, Blackwelder & Haritonidis (1983) demonstrate that the non-dimensional wire length ($l^+ = lu_*/\nu$) strongly influences the mean burst frequency detected by hot-wire probes in the near-wall region. They conclude that when l^+ is larger than 20 significant spatial averaging of the spanwise 'streaky' structure of the wall layer occurs, such that the measured burst frequency is reduced as l^+ is increased. Laboratory studies of bursting in smooth-walled turbulent boundary layers suggest that 65–85 % of the variance of

streamwise velocity fluctuations may be contributed during bursting events (Kim, Kline & Reynolds 1971; Zaric 1974), so it is likely that measurements of $u'/u_* y^+$ in the viscous sublayer may also depend on l^+. Although Blackwelder & Haritonidis (1983) do not discuss this dependence explicitly, they mention that their u' values (at $y^+ = 15$) were typically smaller when measured with longer wires than with shorter wires.

The above findings suggest that the apparent Reynolds-number dependence in Coantic's data may be caused by the increase in l^+ with increasing freestream velocity. His wire length was 0.2 cm (Coantic, personal communication). Inferring u_* from data in Coantic (1966), we estimate that l^+ increased from 16 to 160 as the Reynolds number increased from 50000 to 450000. In contrast, the wire length used for the $Re = 500000$ measurement of Laufer (1954) was 0.025 cm ($l^+ = 18$) (Laufer, personal communication) while the wire length used for the sublayer u' measurements of Comte-Bellot (1965) was 0.04 cm, yielding $l^+ = 36$ at $Re = 230000$ (Comte-Bellot, personal communication). Thus it appears likely that Coantic's apparent Reynolds-number dependence of $u'/u_* y^+$ was caused by the increased spatial averaging of his sensors as l^+ increased from 16 to 160, but that l^+ in the high-Reynolds-number measurements of Laufer and Comte-Bellot was still sufficiently small that spatial averaging did not significantly influence their measurements.

Because there is some reason to doubt the Reynolds-number dependence of Coantic's $u'/u_* y^+$ data, it is unreasonable to attribute the differences between our scaled spectra and those of Bakewell & Lumley (1967) and Ueda & Hinze (1975) to the higher-Reynolds-number range of our field experiment. Furthermore, while the diameter of our heated thermistor bead (0.02 cm) is similar to the hot-wire lengths in the above experiments, the non-dimensional bead diameter du_*/ν was less than 0.5, so it is highly unlikely that spatial averaging influenced our measurements.

If the mean period T_b of the 'bursting' scales with the freestream velocity U_∞ and the boundary-layer thickness δ as suggested by Rao, Narasimha & Badri Narayanan (1971), the reason for the differences between the scaled laboratory and field spectra may be that the mean burst period ($T_b \approx 5\delta/U_\infty$) corresponds to significantly different non-dimensional frequencies ($\hat{\omega} = \omega\nu/u_*^2$) in the field and in the laboratory. The recent study by Blackwelder & Haritonidis (1983), however, demonstrates fairly convincingly that T_b in fact scales with ν/u_*^2 and that the findings of Rao *et al.* were due to the averaging effects of their sensor. If we assume that the scaling of burst period with ν/u_*^2 applies as well to our geophysical flow, then we are forced to dismiss this explanation for the differences between our scaled spectra and those of the laboratory studies.

The lack of complete agreement between the scaled laboratory spectra and those of our study may be related to the fact that, although a viscous sublayer is present at the ocean floor, the boundary between the fluid and the underlying sediment is unlikely to be perfectly flat. Data from another experiment at the same location (Chriss & Caldwell 1983) indicate that the non-dimensional thickness of the viscous sublayer was far more variable than observed in laboratory flows over perfectly smooth walls. Analysis of data from laboratory experiments (Antonia & Luxton 1972; Andreopoulos & Wood 1982; Mulhearn 1978; Chen & Roberson 1974) suggests that this variability may have been related to upstream changes of surface roughness or the presence of distributed roughness elements. These laboratory data indicate that the near-bed flow adjusts very slowly to upstream roughness changes and that profiles in the field may be influenced by roughness effects several metres to tens of metres upstream. The time-lapse ciné camera on the tripod did obtain low-quality photographs

of the seabed, but because the lighting was optimized for monitoring the condition of the sensors and because the field of view was restricted to approximately 1 m^2, the photographs supply little information about upstream conditions. Bottom photographs along the 200 m isobath 65 km south of the studied area (Chriss & Caldwell 1982) indicate the presence of sea urchins and biogenic sediment mounds from a few cm to more than 15 cm high, so roughness effects may have influenced the near-bed spectra. A recent study of the response of atmospheric boundary-layer spectra to changes of terrain (Panofsky *et al.* 1982) indicates that the low-frequency portion of spectra from within internal boundary layers adjusts far more slowly to new boundary conditions than does the high-frequency portion of the spectra; thus the high-frequency portions of the spectrum may be in equilibrium with local conditions, while the low-frequency portion may still reflect upstream conditions. If sublayer and buffer-layer spectra from disturbed smooth-wall boundary layers behave similarly to the logarithmic-layer spectra studied by Panofsky *et al.* then the differences in the shape of our spectra and those of the laboratory may be attributable to upstream topographic changes. To the best of our knowledge, however, sublayer spectral data are not available from disturbed smooth-wall boundary layers, so we cannot evaluate the influence of upstream conditions. It appears that the only relevant sublayer information is the single laboratory u' profile of Mulhearn (1978), from which one can calculate $u'/u_* \, y^+ \approx 0.37$ approximately $25000\nu/u_*$ downstream of a rough-to-smooth transition. Although this suggests that scaled spectra from perturbed smooth-wall boundary layers may contain somewhat more, rather than less, energy than scaled smooth-wall spectra, we cannot conclude from this single measurement that upstream-roughness effects will always increase the energy in the scaled sublayer spectra. Sublayer spectra from laboratory boundary layers with roughness distributions more typical of the sea floor are required for further exploration of this point.

8. Conclusions

Spectra of velocity fluctuations have been determined for the first time in the viscous sublayer and buffer layer of a geophysical boundary-layer flow. The spectral scaling proposed by Bakewell & Lumley (1967) for the viscous sublayer considerably collapses the sublayer spectra from this flow and several laboratory flows. Buffer-layer spectra from $y^+ = 18$ to $y^+ = 29$ collapse reasonably well with laboratory spectra ($y^+ \approx 20$) when frequencies are scaled by $\bar{U}(y)/y$ and spectral densities are scaled by $u_*^2 \, \hat{\omega}/\omega$, where $\hat{\omega}$ is the non-dimensional frequency given by $\omega y/\bar{U}(y)$.

Although this scaling is moderately effective, the non-dimensional spectral densities of the geophysical sublayer and buffer-layer spectra fall below the laboratory spectra in the energy-containing range. This observation could be explained by Reynolds-number effects observed by Coantic (1967), but interpretation of recent work by Blackwelder & Haritonidis (1983) suggests that the Reynolds-number dependence of Coantic's data may be an artifact caused by the spatial averaging of his sensors, and that scaled spectra from high-Reynolds-number flows do not necessarily contain less energy than spectra from lower-Reynolds-number experiments.

Alternatively, the lack of complete agreement of our spectra with the scaled laboratory spectra may be due to the fact that the ocean floor is not perfectly planar. Detailed sublayer measurements in disturbed smooth-walled laboratory boundary layers, as well as detailed information on upstream micro-topography in the field, may be required for the unambiguous interpretation of near-bed spectra.

Particular appreciation is expressed to Priscilla Newberger, Steve Wilcox, Stuart Blood, Mike Brown, Ralph Moore and Stuart Eide, who contributed immensely to the experiment, both at sea and in the laboratory. Dr J. Laufer suggested the possible influence of wire length on the laboratory data, and Drs M. Coantic, G. Comte-Bellot and R. Blackwelder graciously furnished copies of otherwise-unavailable manuscripts. This material is based upon work supported by the National Science Foundation under Grant no OCE-7918904.

REFERENCES

ANDREOPOULOS, J. & WOOD, D. H. 1982 The response of a turbulent boundary layer to a short length of surface roughness. *J. Fluid Mech.* **118**, 143–164.

ANTONIA, R. A. & LUXTON, R. E. 1972 The response of a turbulent boundary layer to a step change in surface roughness. Part 2. Rough-to-smooth. *J. Fluid Mech.* **53**, 737–757.

BATH, M. 1974 *Spectral Analysis in Geophysics.* Elsevier.

BAKEWELL, H. P. & LUMLEY, J. L. 1967 Viscous sublayer and adjacent wall region in turbulent pipe flow. *Phys. Fluids* **10**, 1880–1889.

BLACKWELDER, R. F. & KAPLAN, R. E. 1976 On the wall structure of the turbulent boundary layer. *J. Fluid Mech.* **76**, 89–112.

BLACKWELDER, R. F. & HARITONIDIS, J. H. 1983 Scaling of the bursting frequency in turbulent boundary layers. *J. Fluid Mech.* **132**, 87–104.

CALDWELL, D. R. 1978 Variability of the bottom mixed layer on the Oregon shelf. *Deep-Sea Res.* **25**, 1235–1244.

CALDWELL, D. R. & CHRISS, T. M. 1979 The viscous sublayer at the sea floor. *Science* **205**, 1131–1132.

CALDWELL, D. R. & DILLON, T. M. 1981 An oceanic microstructure measuring system. *Oregon State Univ., School of Oceanogr. Ref.* 81–10.

CHEN, C. K. & ROBERSON, J. A. 1974 Turbulence in wakes of roughness elements. *J. Hydraul. Div. ASCE* **100**, 53–67.

CHRISS, T. M. & CALDWELL, D. R. 1982 Evidence for the influence of form drag on bottom boundary layer flow. *J. Geophys. Res.* **87**, 4148–4154.

CHRISS, T. M. & CALDWELL, D. R. 1983 Universal similarity and the thickness of the viscous sublayer at the ocean floor. *J. Geophys. Res.* in press.

COANTIC, M. 1966 Contribution à l'étude de la structure de la turbulence dans une conduite de section circulaire. Thèse, doctorat d'état des sciences physiques, Université d'Aix-Marseille, Marseille.

COANTIC, M. 1967 Evolution, en fonction du nombre de Reynolds, de la distribution des vitesses moyennes et turbulentes dans une conduite. *C. r. Acad. Sci. Paris* **264A**, 849–852.

COMTE-BELLOT, G. 1965 Ecoulement turbulent entre deux parois parallèles. *Publ. Sci. Tech. Min. Air* no. 149.

DILLON, T. M. & CALDWELL, D. R. 1980 The Batchelor spectrum and dissipation in the upper ocean. *J. Geophys. Res.* **85**, 1910–1916.

ECKELMANN, H. 1974 The structure of the viscous sublayer and the adjacent wall region in a turbulent channel flow. *J. Fluid Mech.* **65**, 439–459.

FORTUNA, G. & HANRATTY, T. J. 1971 Frequency response of the boundary layer on wall transfer probes. *Intl J. Heat Mass Transfer* **14**, 1499–1507.

HANRATTY, T. J. 1967 Study of turbulence close to a solid wall. *Phys. Fluids Suppl.* **10**, S126–S133.

HANRATTY, T. J., CHORN, L. G. & HATZIAVRAMIDIS, D. T. 1977 Turbulent fluctuations in the viscous wall region for Newtonian and drag reducing fluids. *Phys. Fluids suppl.* **20**, S112–S119.

KIM, H. T., KLINE, S. J. & REYNOLDS, W. C. 1971 The production of turbulence near a smooth wall in a turbulent boundary layer. *J. Fluid Mech.* **50**, 133–160.

KLEBANOFF, P. S. 1954 Characteristics in a boundary layer with zero pressure gradient. *NACA TN 3187.*

KREPLIN, H. P. & ECKELMANN, H. 1979 Behavior of the three fluctuating components in the wall region of turbulent channel flow. *Phys. Fluids* **22**, 1233–1239.

LAUFER, J. 1951 Investigation of turbulent flow in a two-dimensional channel. *NACA TR 1053*.

LAUFER, J. 1954 The structure of turbulence in fully developed pipe flow. *NACA TR 1174*.

LAUFER, J. & BADRI NARAYANAN, M. A. 1971 Mean period of the turbulent production mechanism in a boundary layer. *Phys. Fluids* **14**, 182–183.

MITCHELL, J. E. & HANRATTY, T. J. 1966 A study of turbulence at the wall using an electrochemical wall shear-stress meter. *J. Fluid Mech.* **26**, 199–221.

MONIN, A. S. & YAGLOM, A. M. 1971 *Statistical Fluid Mechanics*, vol. 1. MIT Press.

MULHEARN, P. J. 1978 A wind-tunnel boundary-layer study of the effects of a surface roughness change: rough to smooth. *Boundary-Layer Met.* **15**, 3–30.

NEWBERGER, P. A. & CALDWELL, D. R. 1981 Mixing and the bottom nepheloid layer. *Mar. Geol.* **41**, 321–336.

PANOFSKY, H. A., LARKO, D., LIPSCHUTZ, R., STONE, G., BRADLEY, E. F., BOWEN, A. J. & HOJSTRUP, J. 1982 Spectra of velocity components over complex terrain. *Q. J. R. Met. Soc.* **108**, 215–230.

PY, B. 1973 Etude tridimensionnelle de la sous-couche visqueuse dans une veine rectangulaire par des mesures de transfert de matière en paroi. *Intl J. Heat Mass Transfer* **16**, 129–144.

RAO, K. N., NARASIMHA, R. & BADRI NARAYANAN, M. A. 1971 The 'bursting' phenomenon in a turbulent boundary layer. *J. Fluid Mech.* **48**, 339–352.

RUNGE, E. J. 1966 Continental shelf sediments, Columbia River to Cape Blanco, Oregon. Ph.D. thesis, Oregon State University, Corvallis.

SREENIVASAN, K. R. & ANTONIA, R. A. 1977 Properties of wall shear stress fluctuations in a turbulent duct flow. *Trans. ASME* E: *J. Appl. Mech.* **44**, 389–395.

UEDA, H. & HINZE, J. O. 1975 Fine-structure turbulence in the wall region of a turbulent boundary layer. *J. Fluid Mech.* **67**, 125–143.

WALLACE, J. M., BRODKEY, R. S. & ECKELMANN, H. 1977 Pattern-recognized structures in bounded turbulent shear flows. *J. Fluid Mech.* **83**, 673–693.

ZARIC, Z. 1974 Statistical analysis of wall turbulence phenomena. In *Turbulent Diffusion in Environmental Pollution* (ed. F. N. Frenkiel & R. E. Munn); *Adv. Geophys.* **18 A**, 249–261.